R. & M. No. 3459

MINISTRY OF AVIATION

AERONAUTICAL RESEARCH COUNCIL
REPORTS AND MEMORANDA

Experiments Concerning the Effect of Trailing-Edge Thickness on Blade Loss and Turbine Stage Efficiency

By I. H. JOHNSTON, D. C. DRANSFIELD and D. J. FULLBROOK

LONDON: HER MAJESTY'S STATIONERY OFFICE
1967

PRICE 9*s*. 6*d*. NET

Experiments Concerning the Effect of Trailing-Edge Thickness on Blade Loss and Turbine Stage Efficiency

By I. H. JOHNSTON, D. C. DRANSFIELD and D. J. FULLBROOK

Reports and Memoranda No. 3459*
October, 1964

Summary.

Theoretical assessments of the influence of trailing-edge thickness on turbine blade loss coefficients are reviewed and compared with the results of a cascade tunnel investigation. Tests on a single-stage turbine indicate that efficiency is much more sensitive to stator blade trailing-edge thickness than simple estimates would indicate, but rotor blade thickness effects on efficiency are in line with simple prediction.

LIST OF CONTENTS

Section

*Replaces N.G.T.E. Report No. R.264—A.R.C. 26 625.

LIST OF CONTENTS—*continued*

Section

LIST OF ILLUSTRATIONS

Figure

Figure

---

1. *Introduction.*

In the design of turbine blade sections, one feature which inevitably demands some compromise between the rival claims of aerodynamic performance and mechanical integrity is the trailing-edge thickness. While it is unarguable that the lowest loss and hence highest efficiency would be provided by blades with knife-like trailing edges, it is also evident that thin edged blades are ill-suited to withstand the thermal shocks and thermal stresses which are imposed on the blades by the high temperature conditions which are typical of current aircraft gas turbines. A further penalty associated with thin-trailing-edge blades is that they are not amenable to internal cooling due to the impossibility of locating cooling passages within the trailing-edge regions. (This difficulty can however be alleviated by resorting to a film cooling technique for the thin part of the blades).

It is evident that the optimum engineering solution is to select the minimum thickness which the particular operating conditions will permit. However, this is generally somewhat ill-defined, and so it is desirable that the sensitivity of turbine performance to changes in blade trailing-edge thickness should be clearly appreciated.

Needless to say, this question has already received some attention and References 1 and 2 provide theoretical assessments of the influence of trailing-edge thickness on blade loss. However, such assessments are based on certain simplifying assumptions, and for the estimated changes in blade loss to be interpreted as changes in stage efficiency, further assumptions are required.

In view of this it was decided that an experimental evaluation of the influence of trailing-edge thickness on turbine stage efficiency should be made.

Accordingly, a series of stator and rotor blade sections were designed to give progressive variation in trailing-edge thickness. Representative blade cascades were tested to provide a measure of the sensitivity of blade loss to trailing-edge thickness for comparison with estimates based on the analysis of References 1 and 2. Tests were then run on a single-stage turbine to measure the separate influences of stator and rotor blade trailing-edge thicknesses upon turbine stage efficiency.

This report presents a description of the cascade and turbine tests and illustrates the differences between real effects and the predictions of simple theory.

2. *Theoretical Background.*

The effect of trailing-edge thickness upon two-dimensional blade loss has been analysed previously in References 1 and 2 and a summary of this work is indicated in Figure 1.

The method of analysis requires the representation of the blade boundary layer at the trailing-edge plane by a simple power law velocity distribution, the trailing-edge thickness forming a separation distance between the pressure and suction surface boundary layers. It is assumed that uniform flow conditions are achieved at a plane downstream of the trailing edge and the pressure loss from blade inlet to this downstream plane is then evaluated by applying conservation of momentum and continuity of flow between the trailing-edge position and the downstream plane.

The first figure in Figure 1 shows the effect of trailing-edge thickness on blade loss for a range of basic blade loss coefficients, and, as might be expected, the increase in loss with increase in trailing-edge thickness is greatest for the blade having the lowest basic loss.

The second figure illustrates the effect of blade outlet angle. It may be noted that the expansion area ratio between the trailing-edge plane and a downstream station can be represented approximately as $\dfrac{1}{1-\dfrac{t_e}{s\,.\cos\alpha}}$, and at a constant value of $\frac{t_e}{s}$ this expression increases rapidly at the higher values of α. This accounts in part for the increase in sensitivity of loss to thickness as outlet angle increases from 60 deg. to 75 deg.

The method of Reference 1 assumed incompressible flow, but in Reference 2, at the expense of considerable additional complexity, the analysis was extended to include compressible flow. The bottom graph in Figure 1 shows that for a prescribed outlet angle and basic loss coefficient, the sensitivity of loss to trailing-edge thickness is substantially independent of Mach number.

3. *Blade Sections.*

The stator and rotor blade sections which were constructed for this investigation are shown in Figures 2 and 3. The profile shapes were developed using circular arcs, with the final portion of each suction surface formed by a straight line. Four stator blade shapes were defined, to provide a range of t_e/s from 0·0184 to 0·0715. It will be observed that in an attempt to minimise changes in blade row geometry the variations in trailing-edge thickness were obtained by alterations to the suction surface downstream of the passage throat. Thus it was possible to provide considerable variation in trailing-edge thickness while preserving a constant passage shape up to, and beyond, the throat plane.

Three rotor blade sections were constructed and, as shown in Figure 3, tests were made at two values of pitch/chord ratio. As in the case of the stator blades, the changes in trailing-edge thickness were accommodated by alteration to the suction surface downstream of the passage throat.

The blade spacings illustrated in Figures 2 and 3 correspond to the mean diameter (11·25 in.) station within the turbine. For simplicity of manufacture, both the stator and rotor blades were of constant section and untwisted. It was considered from the evidence of previous work[3] that untwisted blades would provide a representative level of performance for the stage loading and diameter ratio of the blade design in question.

Care was taken to ensure that the three rotor blade assemblies were all tipped to give a nominal radial tip clearance of 0·040 inches.

All turbine testing was done with an axial gap of $\frac{1}{2}$ in. between stator trailing edge and rotor leading edge.

4. *Experimental Facilities.*

4.1 *Cascade.*

The high speed cascade tunnel which was used for the cascade part of the investigation is a standard installation, a description of which may be found in Reference 4. For the tests on the stator blades it was not possible to adapt the turbine stators and so extra blades, identical in section to those for the turbine, but increased to 2 in. in length, were manufactured and assembled into eight-bladed cascades. For the rotor blade tests, a slotted cascade sidewall was used which could accept the blade platforms and pin root fixings of the actual turbine blades. Due to the smaller blade height of the turbine it was necessary to provide a tapered insert on each cascade wall to reduce the standard span of 2 in. down to 1·75 inches. The stator blade chord was 1·3 in. and the rotor blade chord 1 in., so that the cascade aspect ratios were 1·53 and 1·75 respectively. Although these are below the 'standard' value of 2·0, there is some recent evidence to suggest that the mid-span performance at this level of aspect ratio is still representative of two-dimensional flow.

4.2. *Turbine.*

The test rig used for the turbine performance evaluation incorporated a modified version of the model turbine described in Reference 3. The turbine comprised a large inlet volute which led into a parallel annulus of 13 in. O.D. and 9·5 in. I.D. containing the stator blades. The rotor blades were unflared and were mounted by pin roots to an overhung disc carried by a shaft running in ball and roller bearings. Following the rotor was a further length of parallel annulus (three to four blade heights) which carried the outlet instrumentation and which led to the exhaust cone and the outlet ducting.

In contrast to the earlier work on this turbine[3], when an air brake was used to absorb power, the turbine was connected to a high speed water brake which was swung in oil-floating trunnion bearings. The latter provided an excellent mounting with negligible friction and the torque measurement was accomplished by a combination of tare weights and a sensitive spring balance.

Air was supplied to the rig at a temperature of about 80°C by a plant compressor which delivered air *via* a variable aftercooler.

5. *Cascade Tests.*

5.1. *Instrumentation.*

The provisions for measurement of cascade loss and outlet angle followed conventional practice. Inlet total pressure P_1 and temperature T_1 were measured by fixed instruments near one side of the inlet section (following check traverses which proved the uniformity of the inlet flow conditions). Outlet total pressure and flow angle were measured by a claw-type pitot yawmeter carried in a remotely controlled traverse gear, details of which are given in Reference 5.

During each traverse the probe was moved in steps of 0·050 in. in a plane parallel to, and approximately 0·15 in. behind, the blade trailing edges. The three blades in the middle of each cascade were traversed, and, to improve accuracy, the peak loss in each blade wake was found by a step-by-step traverse in the wake region. Outside the wake regions, the indicated loss in total pressure was zero.

To limit the extent of the test work, consideration was restricted to zero incidence conditions, and for each cascade, measurements of loss and angle were made at three exit Mach numbers, 0·3, 0·5 and 0·7.

5.2. *Cascade Test Results.*

5.2.1. *Stator blades.* The test results for the four stator cascades are shown in Figure 4. There is a progressive increase in loss with thickness, but for the thickest blades the loss increases abruptly and the outlet angle reduces. It was suspected that this change in performance might be due to a critical boundary-layer condition, as, in a low turbulence tunnel it is necessary always to guard against a misleading result caused by a laminar boundary-layer separation. For this reason a trip wire of 0·001 in. diameter was attached to the suction surface of each blade at a position about $\frac{1}{3}$ chord back from the leading edge. A repeated test of the cascade then yielded the modified values for loss and outlet angle which are shown in Figure 4. It is of interest to note that the chordwise Reynolds number equivalent to the test Mach number of 0·5 at an air temperature of 20 deg. C is $3{\cdot}5 \times 10^5$. Therefore the measured change in blade loss with the addition of the trip wire confirms a level of critical Reynolds number for the thick trailing edge stator blade which is considerably greater than the notional figure of 0·5 to $1{\cdot}0 \times 10^5$ frequently quoted in the literature.

The blade loss relative to that for a t_e/s of 0·02 is plotted against t_e/s in the third graph of Figure 4 and the measured variation of loss is shown to agree very closely with the theoretical estimate derived from Figure 1 for a comparable blade loss and outlet angle.

The gas outlet angles measured for the various cascades showed a somewhat random variation with thickness, but this was due in part to small variations in opening and pitch between the various cascade assemblies. To correct for these, estimates of gas outlet angle were made following the method of Reference 6 which relates gas angle to opening/pitch. The deviations between these estimated angles and the measured values are shown in the last graph of Figure 4 which indicates that the increases in trailing-edge thickness induce progressive reductions in gas outlet angle. However in the thickness range of practical interest, ($t_e/s \leqslant 0{\cdot}05$), the effect of trailing-edge thickness on outlet angle is less than 0·5 deg.

5.2.2. *Rotor blades.* Test results for the rotor blade cascades are shown in Figure 5 for two pitch/chord ratios, 0·72 and 0·60, corresponding to fifty- and sixty-bladed rotors respectively. The first two figures show the losses and outlet angles for the thin and thick trailing-edge profiles set at a pitch/chord ratio of 0·72. It was suspected that the increase in loss at 0·3 Mach number might be a low Reynolds number effect, as, for the test conditions this Mach number corresponds to a Reynolds number of only $1{\cdot}6 \times 10^5$. Accordingly a repeat traverse was made of the thick trailing edge blades with boundary-layer trip wires on the suction surface. As shown in Figure 5, this resulted in a considerable reduction in blade loss at low Mach number, but there was an increase in loss at high Mach number. This is due to the trip wire, in this case 0·005 in. diameter, being too thick and causing a significant wire drag at high Reynolds number.

Tests of the intermediate thickness rotor blade showed it to be particularly susceptible to Reynolds number effects at all Mach numbers. Experiments demonstrated that laminar separation could be suppressed either by a boundary-layer trip wire or by an increase in upstream turbulence using a wire gauze. The unseparated losses were of the same order as those shown in Figure 5, but in view of the need to induce transition at all Mach numbers the results for the intermediate thickness blades are not included in the present analysis.

The cascade performance of the same rotor blades set at the lower pitch/chord ratios of 0·60 are shown in the lower curves of Figure 5. It is of interest to note that while the thin edged blades still show a sensitivity to Mach number, and hence Reynolds number, the loss of the thick blades is virtually constant for the three test conditions.

The comparison between the test performance and theoretical estimates is presented in Figure 6. The test figures are based on measured losses for a Mach number of 0·5 which was the relative velocity most comparable with the conditions of the turbine tests. For both the wide and close pitch blades the measured sensitivity of loss to thickness is less than the calculated value. It will be noted from the comparison of outlet angles that there is a considerable deviation between the measured and estimated values. It seems possible that the apparent insensitivity of blade loss to trailing-edge thickness may be accountable to a degree of separated flow on the suction surface of the thinnest blade which, to some extent, could mask the effect of an increase in blade thickness.

In comparison with the experimental evidence for the stator blades, the data for the rotor blades is somewhat scanty and difficult to interpret. However, the following broad conclusions may be drawn from the cascade test results.

(i) The influence of trailing-edge thickness upon the two-dimensional loss of the family of stator blades agrees closely with theoretical predictions.

(ii) The rotor blade is less sensitive to thickness, the rate of increase in loss being less than the predicted value.

6. *Turbine Tests.*

6.1. *Instrumentation.*

A diagrammatic sketch of the turbine annulus showing the basic instrumentation is given in Figure 7. The main items were as follows:

6.1.1. Turbine inlet total pressure was measured by four pitot tubes set at mean diameter. The local measured value was modified by a calibration constant derived from inlet traverses to give a true mean inlet pressure.

6.1.2. Turbine inlet static pressure was measured by four tappings in the outer wall of the annulus.

6.1.3. Turbine outlet total pressure was measured by four five-point pitot rakes which were coupled together and set to the correct angle by balancing a yawmeter at the mean diameter of each rake.

6.1.4. Turbine outlet static pressure was measured by four outer wall and four inner wall static tappings set in the parallel annulus downstream of the rotor blades.

6.1.5. A small traverse gear carrying a pitot yawmeter was used to provide radial distributions of total pressure and flow angle at turbine exit. In the second series of turbine tests this traverse data was used to provide the flow angles necessary for the calculation of outlet total pressure from measured values of static pressure and mass flow.

6.1.6. Stagnation-shielded thermocouples were used to measure temperature in the inlet volute and downstream of a honeycomb straightener in the exhaust duct.

6.1.7. Air mass flow was measured using a standard BS orifice meter. (The accuracy of this meter has recently been confirmed by flow tests using a calibrating nozzle).

6.1.8. As mentioned in Section 4.2, power was absorbed by a high speed water brake and torque was measured by means of accurate tare weights and a sensitive spring balance.

6.2. *Turbine Test Results.*

6.2.1. *Fifty-bladed rotor.* For the initial performance calibration the turbine was assembled with the thinnest trailing-edge stator and rotor blades, and calibrations were made at three pressure ratios, test measurements being recorded at a number of speed conditions in the range 8,000 to 12,000 rev/min. The stage efficiencies measured with this initial blade assembly are shown in Figure 8a. Keeping the same stator assembly the rotor was then fitted with the thickest trailing edge blades, but no mesurable change in efficiency was detected.

The thin trailing edge rotor blades were reinserted, and the turbine was tested with the two thickest sets of stator blades. The measured efficiencies are compared with the results from the initial build in Figures 8b and 8c.

For each test configuration some additional measurements of flow and pressure ratio were made at a speed ($N/\sqrt{T}$) of 450. The resulting flow characteristics for the various tests are shown in Figure 9a. It will be seen that the change in rotor trailing-edge thickness has no effect on flow, but the thicker nozzles give an increase in flow of 4 to 5 per cent. Inspection figures for the thick trailing edge stator blade rows indicated a throat area approximately 1 per cent greater than for the thin blades and this accounts for about 1 per cent of the observed increase in flow. Reference to the cascade test results (Figure 4) shows that the thicker blades cause a reduction in gas outlet angle of about 1 deg. A simple analysis of stage vectors shows that a reduction of 1 deg. in stator outlet angle from 63·5 deg. to 62·5 deg. is equivalent to an increase in flow of approximately 3 per cent. Thus the change in flow characteristic is accountable to an increase in throat area coupled with a reduction in gas outlet angle.

Traverses of pressure and flow angle were made at turbine exit for each test, and radial distributions of relative flow angle (α_2) and V_a were obtained. These were similar for all the tests and typical distributions are shown in Figure 9b. The momentum mean of the angle distribution is shown to be about 5 deg. lower than the value estimated by the method of Reference 6 on the basis of mean diameter blade shape and allowing for a tip clearance effect. This suggests that the flow separation from the suction surface which was suspected from the cascade results may be even greater in extent within the turbine. This would explain the complete insensitivity of stage performance to the change in rotor blade trailing-edge thickness.

Accordingly the rotor blade root platforms were modified to permit closer pitching and a further series of tests was undertaken.

6.2.2. *Sixty-bladed rotor.* As it was intended to restrict detailed analysis of the effects of trailing-edge thickness to the zero incidence condition a new test technique was used for tests with the sixty-bladed rotor. For each test condition, speed and pressure ratio were adjusted to give the design stage loading of $\dfrac{2kp\Delta T}{u^2} = 3{\cdot}0$ for stage pressure ratios between 0·79 and 0·6.

The first test in this series featured the thinnest stator and rotor blades and the measured efficiency is shown in Figure 10a. In addition to measuring the outlet total pressure directly, as in the previous tests, continuity values of total pressure were calculated on the basis of measured flow, static pressure, total temperature and outlet swirl angle. Test efficiencies derived by each method are shown separately in Figure 10a and it will be observed that the agreement between the two methods of performance assessment is very satisfactory. For all subsequent tests the efficiency was computed by both methods and the plotted characteristics are the best mean lines through all the points. With the thin rotor retained, tests were made using the thicker stator blades, profiles numbers 2 and 3, and test efficiency is compared with that of the thinnest blades in Figures 10b and 10c.

The thin turbine stator blades were then returned to the turbine and tests of the thicker rotor blades, profiles numbers 2 and 3, were carried out. The resultant efficiency characteristics at constant stage loading are shown in Figures 11a and 11b.

Finally to check the additive effect of increasing both the stator and rotor trailing-edge thickness the second stator blades with $t_e/s = 0{\cdot}037$ were assembled with the intermediate rotor blades $t_e/s = 0{\cdot}0502$. The results of this test are shown in Figure 11c. Unfortunately these results exhibited a considerable separation between the efficiencies based on measured and continuity total pressure, the 'measured' efficiency being about 1·5 per cent higher over most of the test range. For this reason it was necessary to depict the test efficiency by a scatter band 1·5 points in width.

The flow characteristics for the various sixty-bladed rotor tests are shown in Figure 12a. Once again although thicker rotors cause no change in flow, there is a marked increase in flow associated with the thicker stator blades.

The radial distribution of blade relative exit angle for the thin rotor is shown in Figure 12b where comparison is made with the distribution for the fifty-bladed rotor. It may be observed that the increase in blade number has increased the relative outlet angle by 5 deg. to 6 deg. to a mean value which is identical with the estimated angle based on opening/pitch. The mean outlet angle for the sixty-bladed thick trailing edge rotor is also shown in Figure 12b and is approximately 2 deg. less than the mean value for the thin blades.

7. *Discussion.*

The results of the tests described in the preceding section are compared in Figure 13. Figure 13a shows stage efficiencies at $\frac{2kp\Delta T}{u^2} = 3{\cdot}0$ for the tests in which stator trailing-edge thickness was varied (the rotor thickness being a minimum throughout). The efficiency for each test is indicated by a scatter band which covers results measured in the pressure ratio range 0·765 to 0·625. It is evident that, for the thinnest blades, the reduction in rotor pitch/chord ratio is accompanied by a significant improvement in efficiency.

Figure 13b illustrates the change in stage efficiency with rotor blade trailing-edge thickness at minimum stator trailing-edge thickness. As mentioned in Section 6.2.1, the increase in rotor t_e/s from 0·0195 to 0·0978 for the fifty-bladed rotor has no significant effect on efficiency, but as the thickness increases from t_e/s of 0·0234 to 0·1170 for the sixty-bladed rotor there is a reduction in stage efficiency of approximately 4 per cent. The insensitivity to thickness at the wider blade pitch suggests that the change in trailing-edge shape must be masked by a region of separated flow. Although the mean diameter rotor blade pitch/chord ratio of the wider pitch build is only 0·72, the Zweifel load coeficient is greater than 1·2, in comparison with typical current design values in the range 0·8 to 1·0, and with such a high aerodynamic loading some degree of flow separation on the suction surface of the blades is not surprising.

In an attempt to generalise the results of the turbine tests, the changes of efficiency due to changes in trailing edge thickness were analysed in terms of blade loss coefficients following the method described in Appendix II and the results of this analysis are shown in Figure 14.

The variations in effective stator loss coefficient with trailing-edge thickness are plotted in Figure 14a and it can be seen that an increase in stator t_e/s from 0·02 to 0·07 causes the effective stator total loss coefficient to rise by a factor of 2·5. This may be compared with a factor of 1·4 derived from the calculated (and measured) variation of loss derived from Figure 4 by the rather dubious assumption of applying a multiplication factor based on two-dimensional flow tests (or calculations) to an overall (three-dimensional) mean loss coefficient. It is clear that this method of assessment seriously underestimates the penalty in effective loss coefficient due to an increase in stator trailing-edge thickness.

Presumably the physical explanation of the sensitivity to trailing-edge thickness must lie in a stator/rotor interaction, such that an increase in stator blade wake induces an additional loss within the rotor blades. In this regard it is of interest to note that the change in rotor pitch/chord ratio does not have a very marked influence on the effective loss coefficient of Figure 14a.

The calculated relative rotor loss coefficients are shown in Figure 14b and for the sixty-bladed assembly there is very good agreement between the variation in loss deduced from turbine results and the calculated variation given in Figure 6. In this case, of course, there is no following blade row to suffer any interaction effects. Although in a multi-stage turbine, the rotor blades would be followed by a row of stator blades, it seems less likely that an interaction as severe as for the stator/rotor situation would occur owing to the normally much wider incidence range of conventional stator blade rows. However, this last comment is purely speculative.

It will be recalled that in the stator blade cascade experiments a very significant increase in loss coefficient was measured in one test; this being attributed to an unexpected laminar separation, and which was subsequently suppressed by means of a boundary-layer trip wire. There was in consequence some speculation as to whether the relatively high apparent stator loss in the turbine tests (revealed by the analysis of Figure 14a) might also have been due to an unexpected laminar separation in the turbine nozzle blades. To check against this, a repeat test of the 0·057 t_e/s stator assembly was carried out with a boundary layer trip wire of 0·001 in. diameter fixed on the suction surface of each of the 36 stator blades. An increase in turbine efficiency of 0·5 per cent was measured which is of the same order as the general accuracy of measurement. This does at least confirm that the marked loss in turbine efficiency with increase in stator blade trailing-edge thickness is not accountable to low-turbulence flow separations from the stator blades.

The final turbine experiment, the result of which is shown in Figure 11c, incorporated a modest increase in trailing-edge thickness for both stator and rotor blades. Relative to the datum blades (t_e/s = 0·0184 and 0·0234) it was deduced from the turbine-based loss data of Figure 14 that the efficiency penalty for blades of t_e/s 0·037 and 0·0502 would be 2·5 per cent. Unfortunately, due to the test result scatter, it is impossible to make an accurate comparison between this estimate and the turbine test result. It is, however, clear that the actual penalty in turbine efficiency is not greater than the effect which can be estimated from turbine-based loss data.

8. *Conclusions.*

(1) The influence of trailing-edge thickness upon turbine blade performance has been examined in cascade experiments and in turbine tests.

(2) For unstalled blades, the increases in measured two-dimensional cascade loss coefficient with thickness are similar to the changes which may be calculated by simple theory.

(3) In a single-stage turbine the effective rotor loss coefficient increases with trailing edge thickness at the same rate as the calculated rate of increase in relative two-dimensional loss coefficient.

(4) The effective stator loss coefficient increases with trailing-edge thickness at a rate which is 1·8 times greater than the calculated rate of increase in relative two-dimensional loss coefficient.

(5) The physical explanation of the sensitivity of stage efficiency to stator trailing-edge thickness is not fully understood. It may however be related to an incidence effect upon the rotor blades and if this is the case it is possible that a turbine stage of higher reaction may be less sensitive to stator trailing-edge thickness.

LIST OF SYMBOLS

α_0	Stator blade gas exit angle
α_1	Rotor blade gas entry angle
α_2	Rotor blade gas exit angle
i	Rotor blade incidence angle
kp	Specific heat at constant pressure
L_N	Stator blade energy loss coefficient
L_R	Rotor blade energy loss coefficient
N	Rotational speed
P_i	Turbine entry total pressure
P_3	Turbine exit total pressure
P_1	Cascade entry total pressure
P_2	Cascade exit total pressure
p_2	Cascade exit static pressure
s	Blade pitch
t_e	Blade trailing-edge thickness
T_i	Turbine entry temperature
ΔT	Turbine stage temperature drop
u	Mean blade speed
Va_1	Axial velocity at rotor entry
Va_2	Axial velocity at rotor exit
λ	Va_2/Va_1
W	Turbine mass flow
Y_N	Stator blade pressure loss coefficient $\left(\frac{P_1-P_2}{P_2-p_2}\right)$
Y_R	Rotor blade pressure loss coefficient

REFERENCES

No.	Author(s)	Title, etc.
1	J. Reeman and E. A. Simonis	The effect of trailing-edge thickness on blade loss. R.A.E. Tech. Note No. Eng. 116. 1943.
2	Warner L. Stewart	Analysis of two-dimensional compressible-flow loss characteristics downstream of turbomachine blade rows in terms of basic boundary-layer characteristics. NACA Tech. Note 3515.'1955.
3	I. H. Johnston and L. R. Knight	Tests of a single-stage turbine comparing the performance of twisted and untwisted rotor blades. A.R.C. R. & M. 2927. February, 1953.
4	A. F. Hounsell	High speed test on a turbine cascade of aerofoil blading, having a maximum profile thickness of 15 per cent chord. ARC 13 557. September, 1950.
5	H. Shaw and H. Ogden	The application of remote control and indication to a high speed cascade tunnel. ARC 13 664. June, 1950.
6	D. G. Ainley and G. C. R. Mathieson	A method of performance estimation of axial flow turbines. A.R.C. R. & M. 2974. December, 1951.
7	I. H. Johnston	An anlysis of the air flow through the nozzle blades of a single-stage turbine. A.R.C. C.P. No. 131. February, 1951.

APPENDIX

Performance Analysis

Consider the fifty-bladed rotor build with thinnest stator and rotor blades.
For the general test pressure ratio level a value for $\lambda = Va_2/Va_1 = 1{\cdot}07$ may be assumed.
Take stator outlet angle $\alpha_0 = 63$ deg.
Take rotor outlet angle $\alpha_2 = 42$ deg. (from Figure 9b)

Let $Va_1/u =$	0·75	0·80	0·85	0·90
$u/Va_1 =$	1·33	1·25	1·176	1·11
$\tan \alpha_1 =$	0·63	0·71	0·784	0·85
$\alpha_1 =$	32·2°	35·4°	38·1°	40·4°
$i =$	−3·8°	−0·6°	+2·1°	+4·4°
$\tan \alpha_1 + \lambda \tan \alpha_2 =$	1·59	1·67	1·74	1·81
$2kp\Delta T/u^2 =$	2·39	2·67	2·96	3·25
Mean η from Figure 8a =	88·8	88·3	87·5	86·5
$\frac{1}{\eta} - 1 =$	0·126	0·133	0·143	0·156

$$\text{Now } \frac{1}{\eta} - 1 = \left(\frac{Va_1}{u}\right)^2 \frac{L_N \sec^2 \alpha_0 + \lambda\, L_R \sec^2 \alpha_2}{\dfrac{2kp\Delta T}{u^2}}$$

where L_N and L_R are the total energy loss coefficients for the stator and rotor blade rows respectively.

Previous experimental work[7] indicates that a representative total pressure loss coefficient Y_N for the thin trailing edge stator blades is 0·06, and at the mean outlet Mach number of the present tests (0·6) the equivalent energy loss coefficient L_N is 0·05.

Solution of the above equation yields values of L_R and corresponding values of Y_R (assuming a rotor exit Mach number of 0·5).

$L_R =$	0·126	0·161	0·177	0·198
$Y_R =$	0·145	0·185	0·205	0·230

Y_R is shown against rotor incidence in Figure 15a.

Turning now to the turbine test results for the thickest trailing-edge stator blades shown in Figure 8c, the modified stator loss coefficient may be assessed as follows:

Take α_0 as 62 deg. to allow for reduction in angle indicated by Figure 4.

α_2 remains at 42 deg.

Let $Va_1/u =$	0·75	0·80	0·85	0·90
$u/Va_1 =$	1·33	1·25	1·176	1·11
$\tan \alpha_1 =$	0·55	0·63	0·704	0·77
$\alpha_1 =$	29·9°	32·2°	35·2°	37·6°
$i =$	−7·1°	−3·8°	−0·8°	+1·6°
$\tan \alpha_1 + \lambda \tan \alpha_2 =$	1·51	1·59	1·664	1·73
$2kp\Delta T/u^2 =$	2·27	2·54	2·83	3·11
Mean η from Figure 8c =		82	81·6	81·0

$\frac{1}{\eta} - 1 =$	0·22	0·226	0·235
(from Figure 15a) $Y_R =$	0·145	0·182	0·203
$L_R =$	0·128	0·164	0·180
Hence $L_N =$	0·129	0·119	0·115

Ideally, as incidence to the stator blades is constant, and if there were no stator/rotor interactions, the above values of L_N should be constant.

Adopting a mean value of 0·121, the equivalent pressure loss coefficient for a Mach number of 0·6 is $Y_N = 0{\cdot}145$.

Therefore the increase in stator t_e/s from 0·0184 to 0·0715 has caused an increase in *effective* stator loss from 0·06 to 0·145, a factor of 2·4. This may be compared with the factor of $\frac{1{\cdot}4}{0{\cdot}96} = 1{\cdot}46$ for the increase in profile loss coefficient shown in Figure 4.

The above method makes allowance for change in stator angle and the consequent variation in the incidence/stage loading relationship indicated in Figure 15b. It is however possible to use a simpler approach which neglects second order effects, but appears adequate for present purposes.

Consider the thin trailing edge assembly for which $\alpha_0 = 63$ deg. and $\alpha_2 = 42$ deg.

For a stage loading $\frac{2kp\Delta T}{u^2}$ of 2·96, the initial analysis shows that,

$$\frac{1}{\eta} - 1 = 0{\cdot}244\,(4{\cdot}85\, L_N + 0{\cdot}342)$$

Now at the same stage loading, the thick stator blades yield an efficiency of 81·3 per cent.

From the above equation, $L_N = 0{\cdot}125$ compared with the mean value of 0·121 deduced previously.

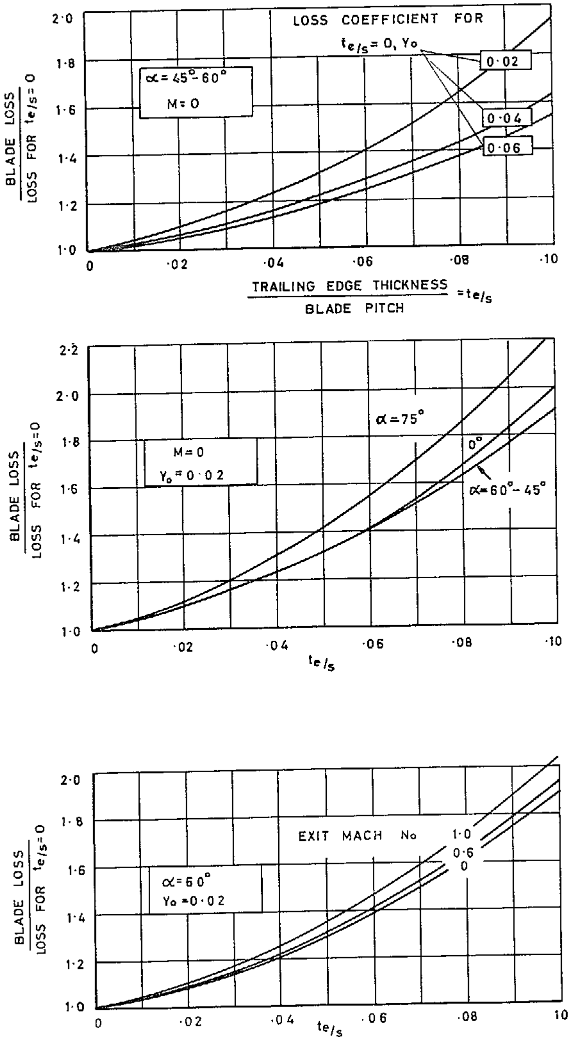

FIG. 1. Calculated effects of trailing-edge thickness on 2-dimensional blade pressure-loss coefficients.

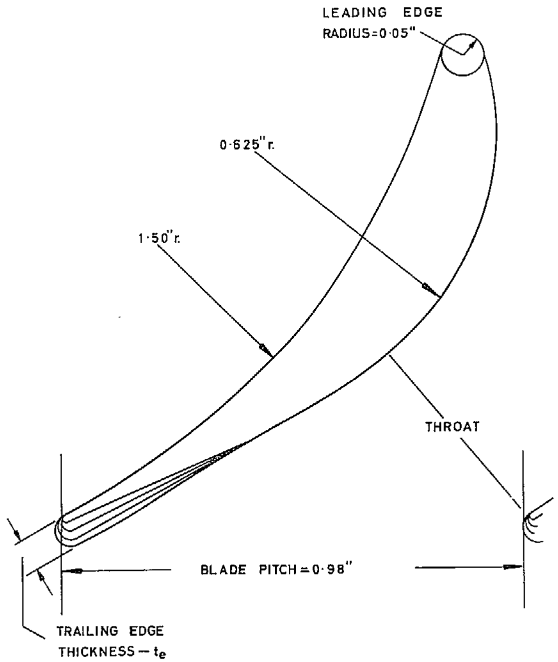

PROFILE	1	2	3	4
t_e"	0·018	0·036	0·056	0·070
t_e/s	0 0184	0·037	0·057	0·0715

FIG. 2. Stator blade profiles.

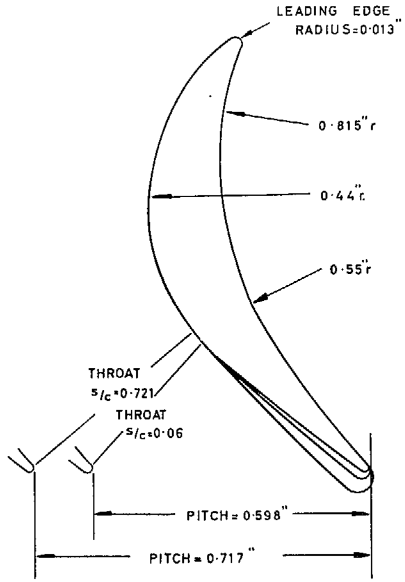

	PROFILE	1	2	3
	t_e"	0·014	0·030	0·070
50 BLADES	t_e/s	0·0195	0·0419	0·0978
60 BLADES	t_e/s	0·0234	0·0502	0·1170

FIG. 3. Rotor blade profiles.

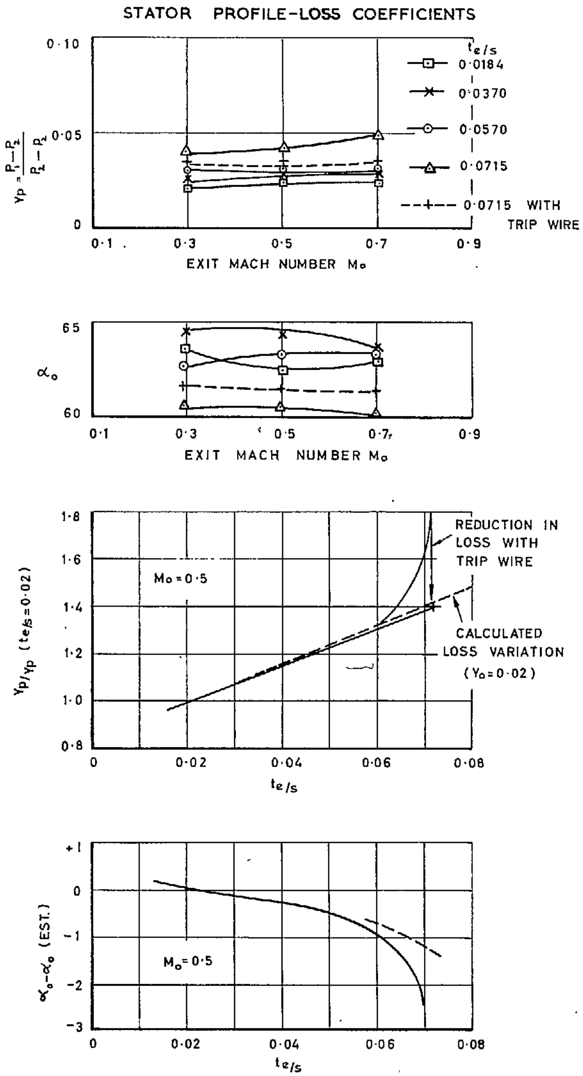

FIG. 4. Stator blades–cascade test results.

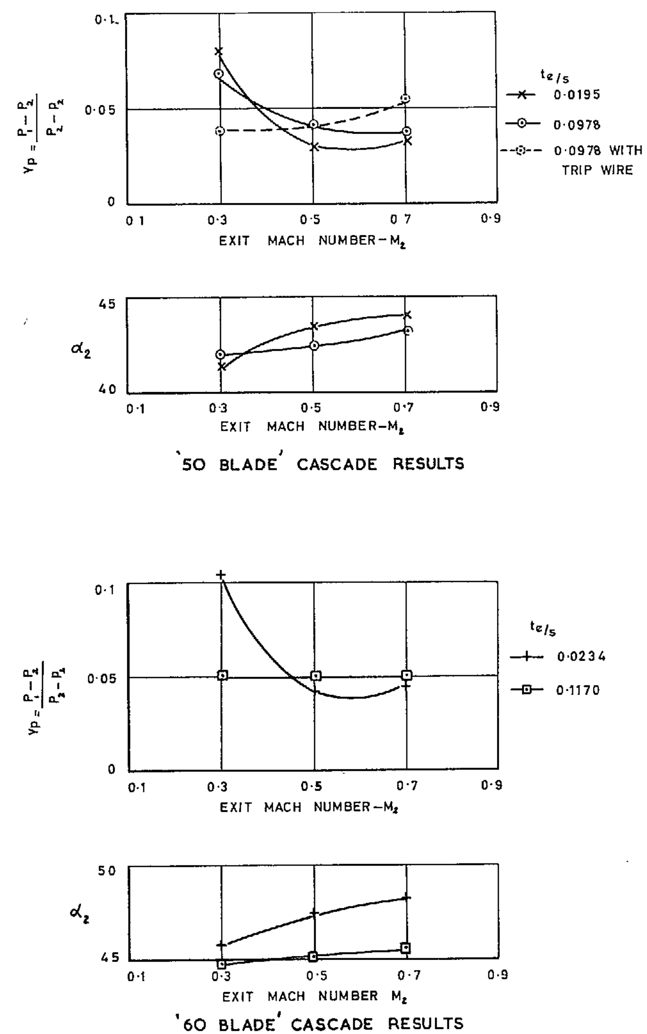

FIG. 5. Rotor blades–cascade test results.

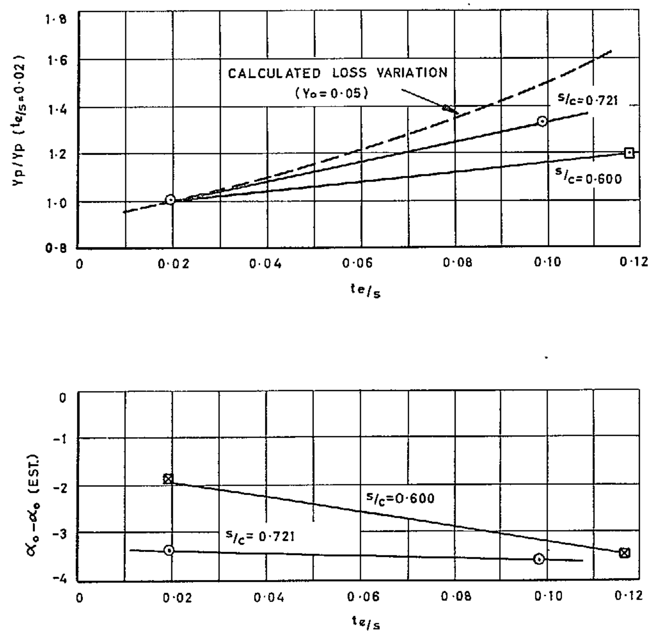

FIG. 6. Rotor blades–cascade test results.

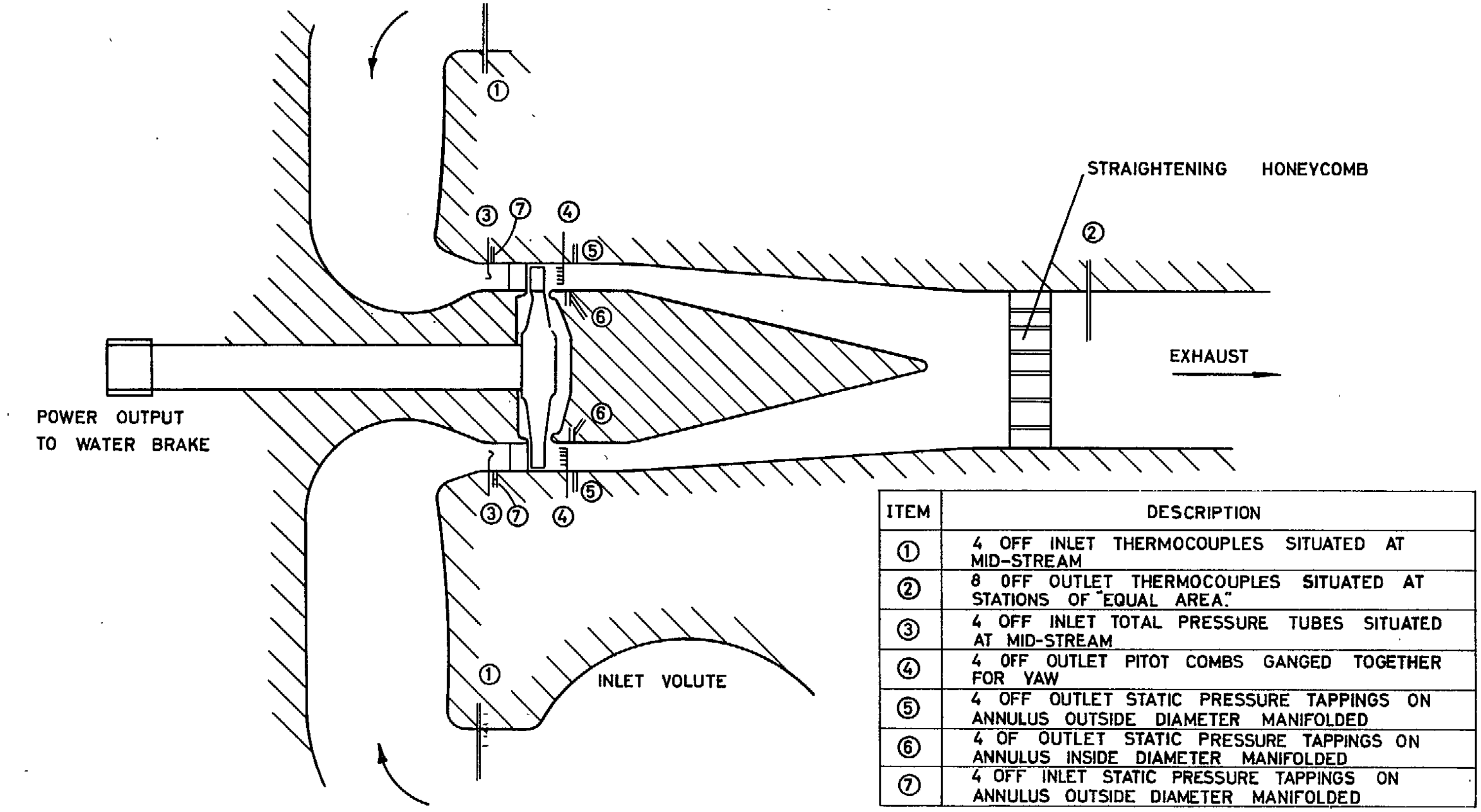

ITEM	DESCRIPTION
1	4 OFF INLET THERMOCOUPLES SITUATED AT MID-STREAM
2	8 OFF OUTLET THERMOCOUPLES SITUATED AT STATIONS OF "EQUAL AREA"
3	4 OFF INLET TOTAL PRESSURE TUBES SITUATED AT MID-STREAM
4	4 OFF OUTLET PITOT COMBS GANGED TOGETHER FOR YAW
5	4 OFF OUTLET STATIC PRESSURE TAPPINGS ON ANNULUS OUTSIDE DIAMETER MANIFOLDED
6	4 OF OUTLET STATIC PRESSURE TAPPINGS ON ANNULUS INSIDE DIAMETER MANIFOLDED
7	4 OFF INLET STATIC PRESSURE TAPPINGS ON ANNULUS OUTSIDE DIAMETER MANIFOLDED

FIG. 7. Schematic arrangement of turbine annulus and instrumentation.

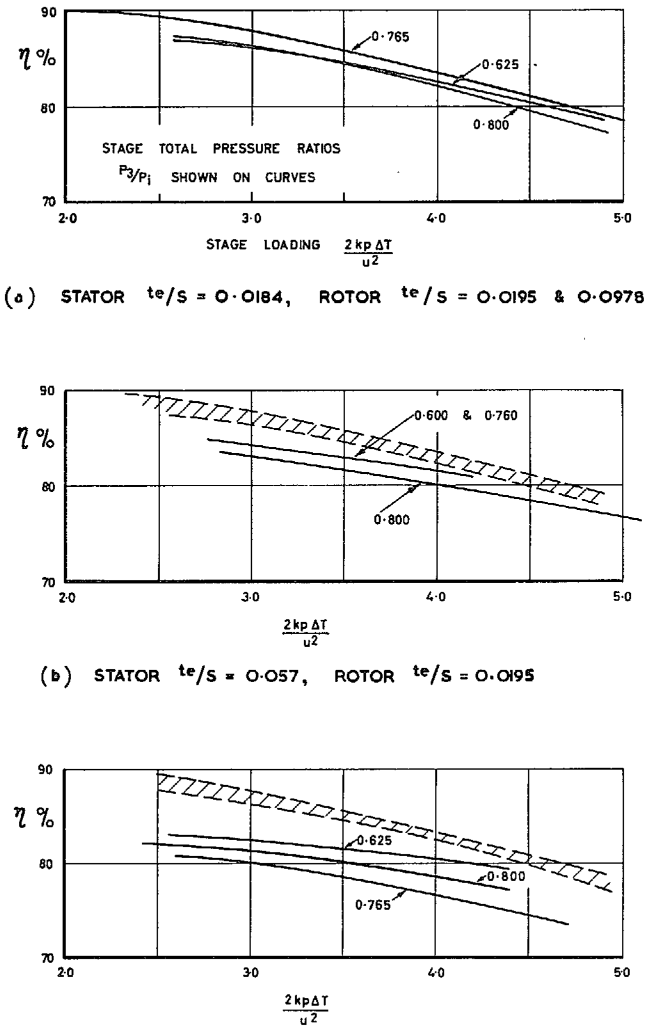

FIG. 8. Test efficiencies. (50-bladed rotor). (Constant pressure ratio characteristics).

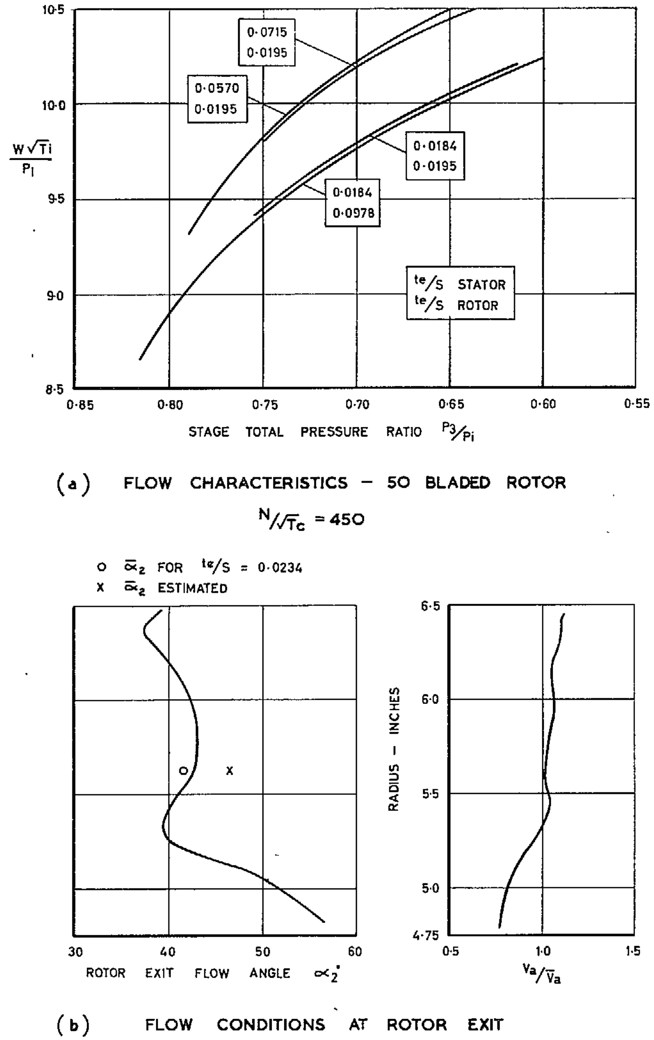

FIG. 9. Test flows and traverse results. (50-bladed rotor).

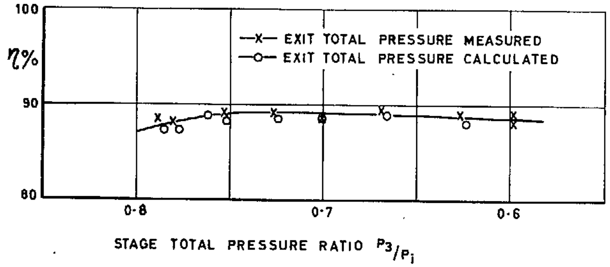

(a) STATOR $te/s = 0{\cdot}0184$ ROTOR $te/s = 0{\cdot}0234$

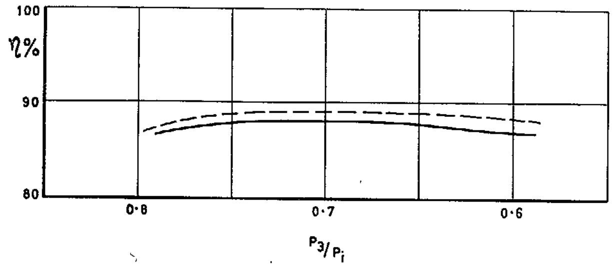

(b) STATOR $te/s = 0{\cdot}037$ ROTOR $te/s = 0{\cdot}0234$

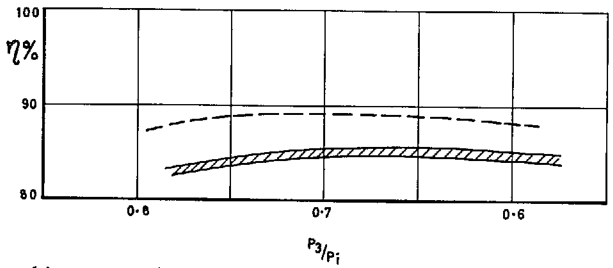

(c) STATOR $te/s = 0{\cdot}057$ ROTOR $te/s = 0{\cdot}0234$

FIG. 10. Test efficiencies. 60-bladed rotor test condition $\dfrac{2kp\Delta T}{U^2} = 3{\cdot}0$.

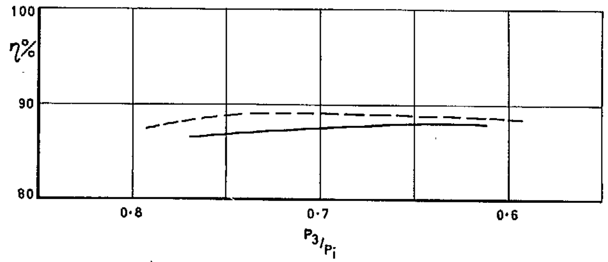

(a) STATOR $te/s = 0{\cdot}0184$ ROTOR $te/s = 0{\cdot}0502$

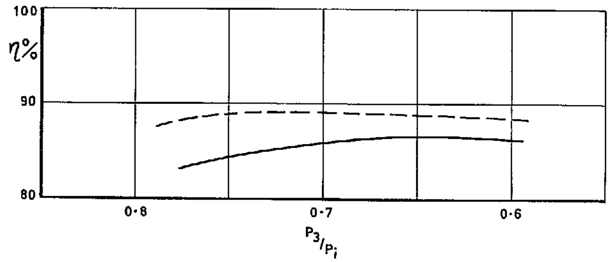

(b) STATOR $te/s = 0{\cdot}0184$ ROTOR $te/s = 0{\cdot}1170$

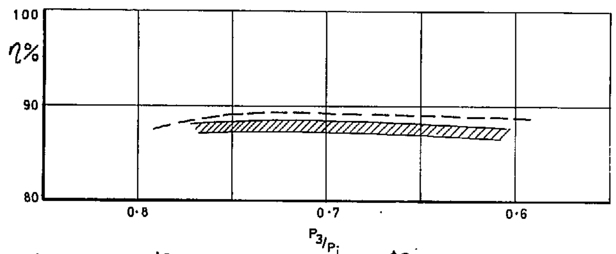

(c) STATOR $te/s = 0{\cdot}037$ ROTOR $te/s = 0{\cdot}0502$

FIG. 11. Test efficiencies. 60-bladed rotor test condition $\dfrac{2kp\Delta T}{U^2} = 3{\cdot}0$.

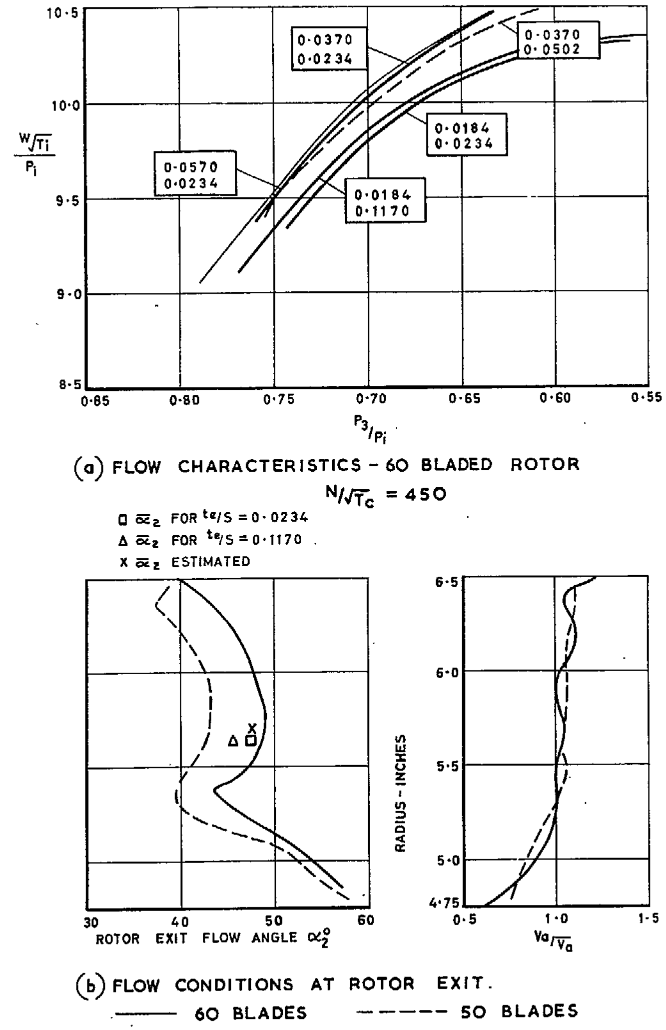

FIG. 12. Test flows and traverse results. (60-bladed rotor).

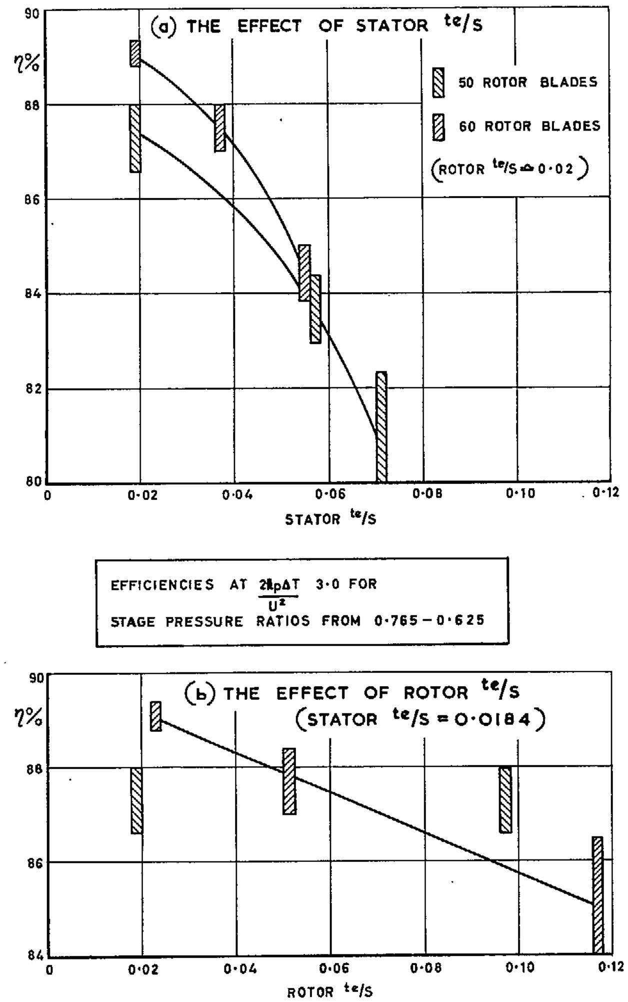

FIG. 13. The influence of trailing-edge thickness on turbine stage efficiency.

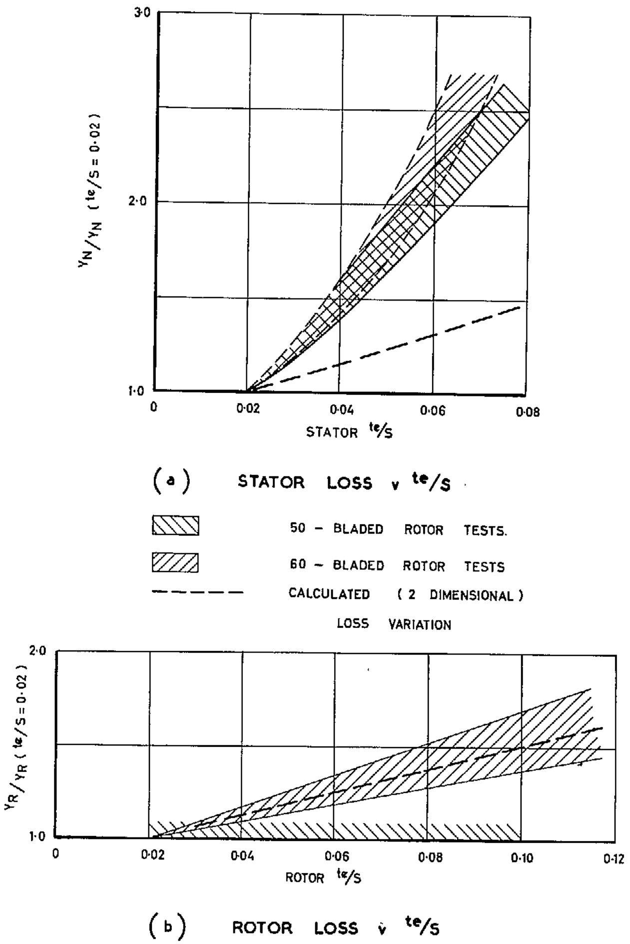

FIG. 14. Blade loss coefficients assessed from turbine test results.

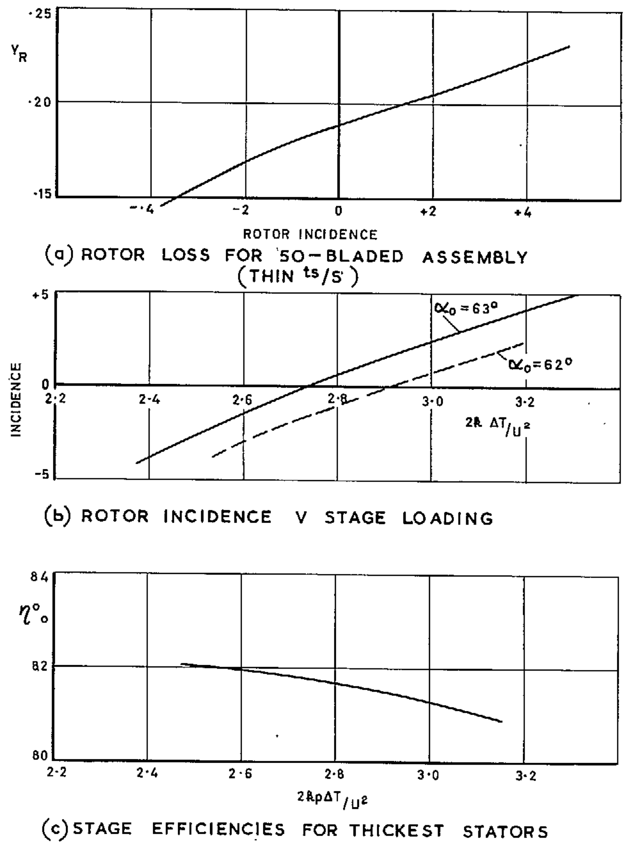

FIG. 15. Performance analysis. (Appendix).

Printed in Wales for Her Majesty's Stationery Office by Allens (Cardiff) Limited

Dd.125874 K5 3/67

Published by
HER MAJESTY'S STATIONERY OFFICE

To be purchased from
49 High Holborn, London W.C.1
423 Oxford Street, London W.1
13A Castle Street, Edinburgh 2
109 St. Mary Street, Cardiff
Brazennose Street, Manchester 2
50 Fairfax Street, Bristol 1
35 Smallbrook, Ringway, Birmingham 5
7–11 Linenhall Street, Belfast 2
or through any bookseller